Electronic Journal of Differential Equations, Vol. 2026 (2026), No. 25, pp. 1–17.
ISSN: 1072-6691. URL: https://ejde.math.txstate.edu, DOI: 10.58997/ejde.2026.25

GLOBAL DYNAMICS OF A MODIFIED HYBRID VAN DER POL-RAYLEIGH OSCILLATOR II

YUHUAN LU, RUI ZHANG

Abstract. In this article, we study a modified hybrid Van der Pol-Rayleigh oscillator. We consider bifurcation diagrams and global phase portraits in the Poincaré disc under some restrictions on the parameters. The resulting bifurcation diagram is complex, containing one saddle-node bifurcation surface at infinity, one cusp bifurcation surface, one Hopf bifurcation surface, and two generalized heteroclinic bifurcation surfaces.

1. Introduction and main results

Nonlinear oscillators arise in numerous fields of applied science and engineering, including mechanical systems, physics, chemistry, and biodynamics, see for instance [1, 2, 4, 8, 15, 16, 17, 18, 19, 20]. The study of self-sustained oscillations, pioneered by van der Pol [18] and Rayleigh [17], has evolved to encompass more complex hybrid models capable of simulating intricate dynamical behaviors, such as those found in bipedal locomotion and pedestrian walking forces, see [9, 10, 11, 12, 13] and references therein.

A typical model is the modified hybrid van der Pol-Rayleigh oscillator [3, 9], equivalent to the planar system

$$\frac{dx}{dt} = y, \quad \frac{dy}{dt} = -x - a_1 y - (a_2 x^2 + a_3 xy + a_4 y^2)y, \tag{1.1}$$

where $a_2 > 0$, $a_4 > 0$ and $a_1 < 0$. This system generalizes classical oscillators and exhibits richer bifurcation phenomena and limit cycle structures. To fully explore its parameter space, particularly for Hopf bifurcation analysis, constraints on the parameters are relaxed to $a_2 \geq 0$, $a_4 \geq 0$ and $a_1 \in \mathbb{R}$. Recent work by Chen et al. [7] established the global dynamics for the case $a_3 = 0$. When $a_3 \neq 0$, under the scaling $(x, y) \to (|a_3|^{-1/2}x, |a_3|^{-1/2}y)$, system (1.1) naturally splits into two topologically distinct families:
Case $a_3 > 0$:

$$\begin{aligned} \frac{dx}{dt} &= y, \\ \frac{dy}{dt} &= -x - ay - (\alpha x^2 + xy + \beta y^2)y, \end{aligned} \tag{1.2}$$

Case $a_3 < 0$:

$$\begin{aligned} \frac{dx}{dt} &= y := P(x, y), \\ \frac{dy}{dt} &= -x - ay - (\alpha x^2 - xy + \beta y^2)y := Q(x, y), \end{aligned} \tag{1.3}$$

where $\alpha \geq 0$, $\beta \geq 0$ and $a \in \mathbb{R}$. We note that the bifurcation diagram and all global phase portraits in the Poincaré disc of system (1.2) have been presented completely in [3]. Naturally, we ask whether the global dynamics of system (1.2) and system (1.3) are topologically equivalent? This is the main motivation for the present study.

2020 *Mathematics Subject Classification.* 34C07, 34C15, 37G15.
Key words and phrases. Van der Pol-Rayleigh oscillator; bifurcation; phase portrait; limit cycle.

Submitted December 22, 2025. Published March 31, 2026.

We start with the bifurcation diagram and all global phase portraits in the Poincaré disc of system (1.3) and demonstrate that the global dynamics of system (1.3) are more intricate than those of system (1.2). Let Ω be the parameter space and

$$\Omega : (\alpha, \beta, a) \in [0, +\infty) \times [0, +\infty) \times \mathbb{R}.$$

Our main results read as follows.

Theorem 1.1. *System* (1.3) *exhibits one finite equilibrium* $O(0,0)$ *and fourteen possible infinite equilibria* $I_A^{\pm}$, $I_B^{\pm}$, $I_C^{\pm}$, $I_D^{\pm}$, $I_E^{\pm}$, $I_F^{\pm}$, $I_G^{\pm}$ *in the Poincaré disc, where* $I_A^{\pm}$ *lie on* $y = \frac{1+\sqrt{1-4\alpha\beta}}{2\beta}x$, $I_B^{\pm}$ *lie on* $\frac{1-\sqrt{1-4\alpha\beta}}{2\beta}x$, $I_E^{\pm}$ *lie on* $y = \alpha x$, $I_F^{\pm}$ *lie on* $y = \frac{1}{\beta}x$, $I_G^{\pm}$ *lie on* $y = \frac{1}{2\beta}x$, $I_C^{\pm}$ *lie on* x*-axis and* $I_D^{\pm}$ *lie on the* y*-axis. Moreover, system* (1.3) *has at most one limit cycle.*

The global bifurcation diagrams of system (1.3) *consist of the following bifurcation surfaces and curves:*

(a) *the saddle-node bifurcation surface at infinity,*

$$SN := \{(\alpha, \beta, a) \in \Omega : \alpha\beta = 1/4\},$$

(b) *the cusp bifurcation (or degenerate saddle-node bifurcation) curve at infinity,*

$$C := \{(\alpha, \beta, a) \in \Omega : \alpha\beta = 1/4, a = -(4\beta^2 + 1)/2\beta\},$$

(c) *the Hopf bifurcation surface,*

$$H := \{(\alpha, \beta, a) \in \Omega : a = 0\},$$

(d) *the Generalized heteroclinic bifurcation curve,*

$$S := \{(\alpha, \beta, a) \in \Omega : \alpha > 0, \beta = 0, a < 0, a + \alpha = 0\},$$

(e) *the Generalized heteroclinic bifurcation curve,*

$$HL := \{(\alpha, \beta, a) \in \Omega : \alpha = 0, \beta > 0, a < 0, a + \beta = 0\}.$$

Moreover, the slice $\alpha = \alpha^*$ *of bifurcation diagrams in* $\Omega \setminus \{(\alpha, \beta, a) : a < 0, 0 < \alpha\beta < 1/4\}$ *is shown in Figure 1. The corresponding global phase portraits in the Poincaré disc of* (1.3) *for the case* $\alpha^* > 0$ *(see Figure 1(a)) are shown in Figure 2(a-k), and for the case* $\alpha^* = 0$ *(see Figure 1(b)) are shown in Figure 2(l-r). There* $\alpha^* \geq 0$ *is a fixed value satisfying the following:*

$$\begin{aligned}
L_1 &= \{(\alpha, \beta, a) \in \Omega : \alpha = \alpha^* > 0, \beta = 0, a \geq 0\},\\
L_2 &= \{(\alpha, \beta, a) \in \Omega : \alpha = \alpha^* > 0, \beta = 0, a < 0, a + \alpha > 0\},\\
L_3 &= \{(\alpha, \beta, a) \in \Omega : \alpha = \alpha^* > 0, \beta = 0, a < 0, a + \alpha < 0\},\\
L_4 &= \{(\alpha, \beta, a) \in \Omega : \alpha = \alpha^* = 0, \beta = 0, a > 0\},\\
L_5 &= \{(\alpha, \beta, a) \in \Omega : \alpha = \alpha^* = 0, \beta = 0, a < 0\},\\
I &= \{(\alpha, \beta, a) \in \Omega : \alpha = \alpha^* > 0, 0 < \beta < 1/4\alpha^*, a \geq 0\},\\
II &= \{(\alpha, \beta, a) \in \Omega : \alpha = \alpha^* > 0, 0 < \beta < 1/4\alpha^*, a < 0\},\\
III &= \{(\alpha, \beta, a) \in \Omega : \alpha = \alpha^* > 0, \beta > 1/4\alpha^*, a \geq 0\},\\
IV &= \{(\alpha, \beta, a) \in \Omega : \alpha = \alpha^* > 0, \beta > 1/4\alpha^*, a < 0\},\\
V &= \{(\alpha, \beta, a) \in \Omega : \alpha = \alpha^* = 0, \beta > 0, a \geq 0\},\\
VI &= \{(\alpha, \beta, a) \in \Omega : \alpha = \alpha^* = 0, \beta > 0, a < 0, a + \beta > 0\},\\
VII &= \{(\alpha, \beta, a) \in \Omega : \alpha = \alpha^* = 0, \beta > 0, a < 0, a + \beta < 0\},\\
SN_1 &= \{(\alpha, \beta, a) \in \Omega : \alpha = \alpha^* > 0, \beta = 1/4\alpha^*, a > 0\} \subset SN,\\
SN_2 &= \{(\alpha, \beta, a) \in \Omega : \alpha = \alpha^* > 0, \beta = 1/4\alpha^*, -(4\beta^2 + 1)/2\beta < a \leq 0\} \subset SN,\\
SN_3 &= \{(\alpha, \beta, a) \in \Omega : \alpha = \alpha^* > 0, \beta = 1/4\alpha^*, a < -(4\beta^2 + 1)/2\beta\} \subset SN,\\
S &= \{(\alpha, \beta, a) \in \Omega : \alpha = \alpha^* > 0, \beta = 0, a < 0, a + \alpha = 0\},\\
C &= \{(\alpha, \beta, a) \in \Omega : \alpha = \alpha^* > 0, \beta = 1/4\alpha^*, a = -(4\beta^2 + 1)/2\beta\} \subset SN,
\end{aligned}$$

$$O = \{(\alpha, \beta, a) \in \Omega : \alpha = \alpha^* = 0, \beta = 0, a = 0\},$$
$$HL = \{(\alpha, \beta, a) \in \Omega : \alpha = \alpha^* = 0, \beta > 0, a < 0, a + \beta = 0\}.$$

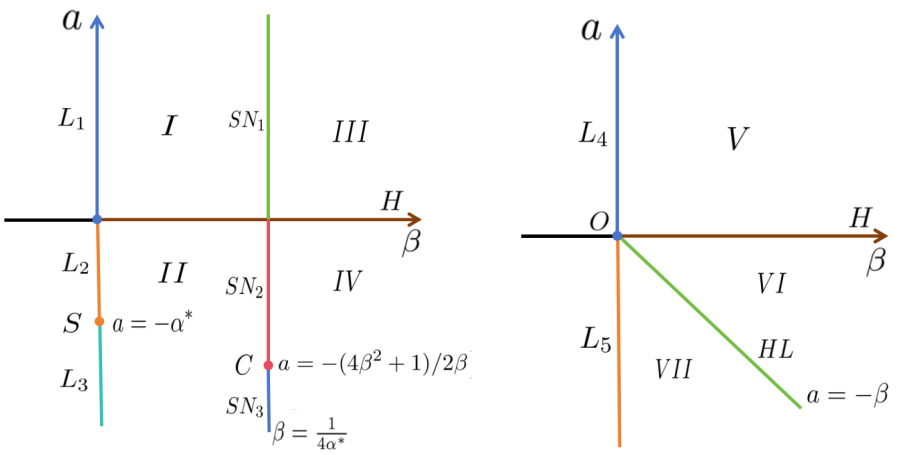

(a) $\alpha^* > 0$ (b) $\alpha^* = 0$

FIGURE 1. The slice $\alpha = \alpha^*$ of the bifurcation diagrams of system (1.3).

Remark 1.2. Note that Theorem 1.1 considers the bifurcation diagrams and global phase portraits of system (1.3) only for parameters in $\Omega \setminus \{(\alpha, \beta, a) : a < 0,\ 0 < \alpha\beta < 1/4\}$. In fact, the exact number of limit cycles remains unknown for system (1.3) when $a < 0$ and $0 < \alpha\beta < 1/4$. In other words, we do not know whether there exist any bifurcation curves associated with limit cycles in II, as shown in Figure 1(a).

The remainder of this article is organized as follows. We analyze the local dynamics of system (1.3) and the Hopf bifurcation in Section 2. We prove the uniqueness of the limit cycle for system (1.3) in Section 3. We prove our main results in Section 4. We compare the global dynamics of systems (1.2) and (1.3), and provide further clarification on limit cycles of system (1.3) with $(\alpha, \beta, a) \in \{(\alpha, \beta, a) : a < 0, 0 < \alpha\beta < 1/4\}$ in Section 5.

2. Local dynamics of system (1.3)

In this section, we study the local dynamical behavior of system (1.3). The first two lemmas focus on the analysis of equilibria at finite points and at infinity, respectively.

Lemma 2.1. *There is a unique equilibrium of system* (1.3)*, denoted by* $O(0, 0)$*. Moreover,*

(i) $O(0, 0)$ *is an unstable focus (resp. node) if* $-2 < a < 0$ *(resp.* $a \le -2$*);*
(ii) $O(0, 0)$ *is a stable focus (resp. node) if* $0 < a < 2$ *(resp.* $a \ge 2$*);*
(iii) $O(0, 0)$ *is a stable weak focus of order one if* $a = 0$ *and* $\alpha^2 + \beta^2 \ne 0$*; and*
(iv) $O(0, 0)$ *is a center if* $a = 0$ *and* $\alpha = \beta = 0$*.*

Proof. By solving $P(x, y) = Q(x, y) = 0$, we obtain that system (1.3) has a unique equilibrium $O(0, 0)$. The Jacobian matrix of system (1.3) at O is

$$\begin{pmatrix} 0 & 1 \\ -1 & -a \end{pmatrix},$$

whose eigenvalues are $\lambda_{1,2} = (-a \pm \sqrt{a^2 - 4})/2$. Thus, it is easy to determine the type of O when $a \ne 0$, see statements (i) and (ii). When $a = 0$, $\lambda_{1,2}$ are a pair of conjugate pure imaginary numbers,

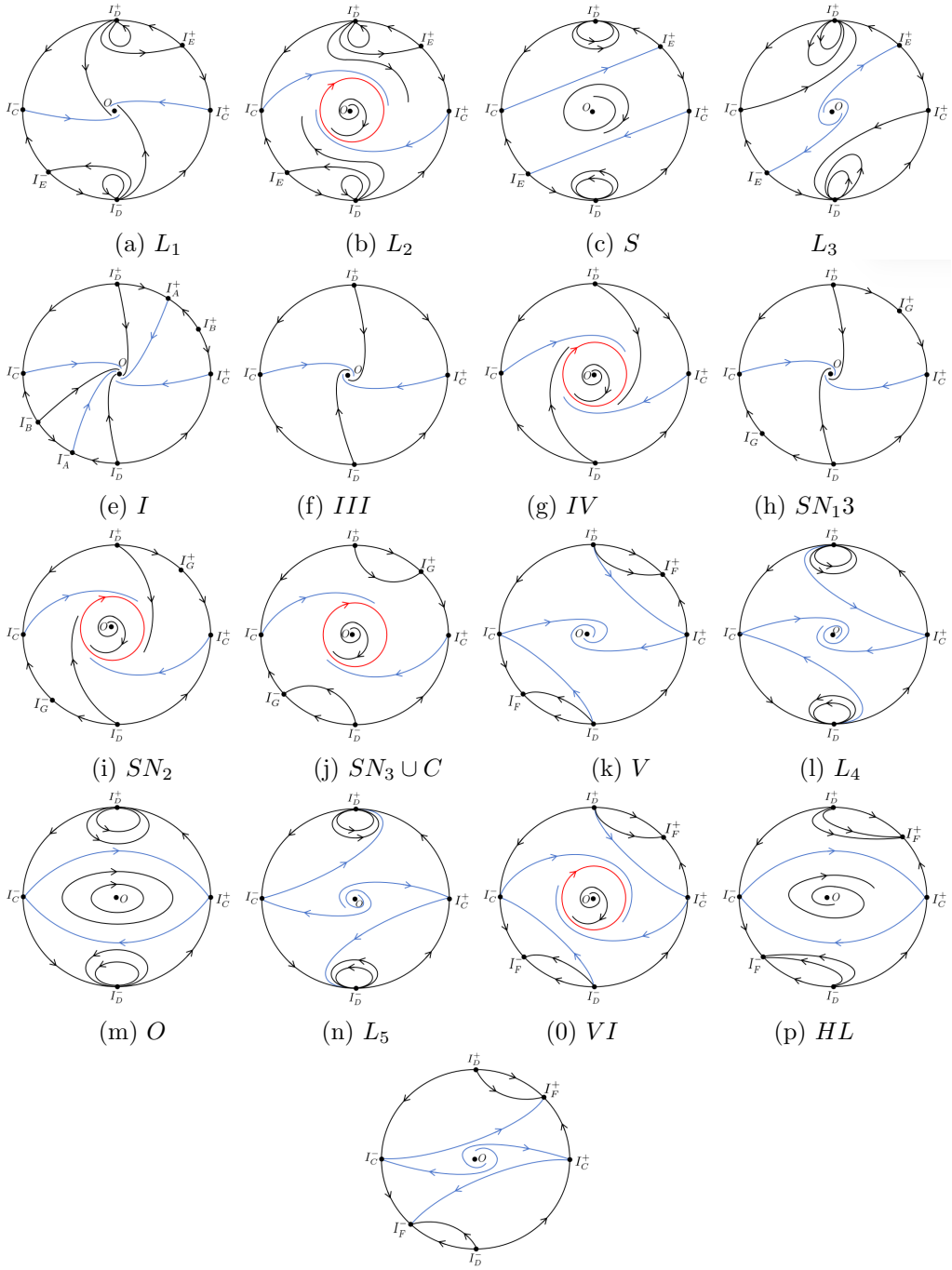

(a) L_1 (b) L_2 (c) S L_3

(e) I (f) III (g) IV (h) $SN_1 3$

(i) SN_2 (j) $SN_3 \cup C$ (k) V (l) L_4

(m) O (n) L_5 (0) VI (p) HL

(q) VII

FIGURE 2. Global phase portraits in the Poincaré disc of system (1.3).

which implies that equilibrium O is either a center or a focus. Using the polar coordinates, $x = r\cos\theta$ and $y = r\sin\theta$, system (1.3) becomes

$$\begin{aligned} \frac{dr}{dt} &= -r^3 \sin^2\theta \left(\beta \sin^2\theta - \cos\theta \sin\theta + \alpha \cos^2\theta\right), \\ \frac{d\theta}{dt} &= -1 - r^2 \sin\theta\cos\theta \left(\beta \sin^2\theta - \cos\theta \sin\theta + \alpha \cos^2\theta\right). \end{aligned} \tag{2.1}$$

Consider the small neighborhood of $O(0,0)$, that is, $0 < r \ll 1$. From (2.1) we obtain

$$\frac{dr}{d\theta} = \frac{r^3 \sin^2\theta \left(\beta \sin^2\theta - \cos\theta \sin\theta + \alpha \cos^2\theta\right)}{1 + r^2 \sin\theta\cos\theta \left(\beta \sin^2\theta - \cos\theta \sin\theta + \alpha \cos^2\theta\right)} = M_3(\theta) r^3 + \mathscr{O}(r^5),$$

where

$$M_3(\theta) = \sin^2\theta \left(\beta \sin^2\theta - \cos\theta \sin\theta + \alpha \cos^2\theta\right).$$

From the formulas for the focal values in [21, Section 5, Chapter 2], we obtain the first focal value

$$g_3 = -\frac{\int_0^{2\pi} M_3(\theta)\, d\theta}{2\pi} = -\frac{3}{8}\beta - \frac{1}{8}\alpha.$$

From $\alpha \geq 0$ and $\beta \geq 0$, $g_3 < 0$ if and only if $\alpha^2 + \beta^2 \neq 0$. Thus, $O(0,0)$ is a stable weak focus of order one if and only if $\alpha^2 + \beta^2 \neq 0$. Hence, statement (iii) is true. Furthermore, when $\alpha = \beta = 0$, we observe

$$P(x,y) = -P(x,-y), \quad Q(x,y) = Q(x,-y),$$

so the vector field of system (1.3) is symmetric with respect to the x-axis. That is, O is a center when $\alpha = \beta = 0$ according to [21, Section 5, Chapter 2] and statement (iv) is obtained. □

To discuss the Hopf bifurcation that appear in a small neighbourhood of the weak focus O in system (1.3), with the aim of determining the number of limit cycles that can emerge, we can obtain the lemma directly by [7, Theorem 2.4 of Chapter 3].

Lemma 2.2. *When $\alpha^2 + \beta^2 \neq 0$, there is a sufficiently small $\varepsilon > 0$ and a small neighborhood $U(O)$ of O such that*

(1) *there is exactly one limit cycle in $U(O)$ of system (1.3) for $-\varepsilon < a < 0$, which is stable; and*
(2) *there are no closed orbits in $U(O)$ of system (1.3) for $0 < a < \varepsilon$.*

To study the dynamics of system (1.3) at infinity along the x-direction and y-direction, we take the Poincaré transformations

$$(x,y) = \Big(\frac{1}{z}, \frac{u}{z}\Big) \quad \text{and} \quad (x,y) = \Big(\frac{v}{z}, \frac{1}{z}\Big),$$

respectively. Then, (1.3) is transformed to

$$\begin{aligned} \frac{du}{d\tau} &= -z^2(u^2 + au + 1) - u(\beta u^2 - u + \alpha), \\ \frac{dz}{d\tau} &= -z^3 u, \end{aligned} \tag{2.2}$$

and

$$\begin{aligned} \frac{dv}{d\tau} &= z^2(v^2 + av + 1) + v(\alpha v^2 - v + \beta), \\ \frac{dz}{d\tau} &= z^3(v + a) + z(\alpha v^2 - v + \beta), \end{aligned} \tag{2.3}$$

where $d\tau = dt/z^2$. For system (2.2) we have the following result.

Lemma 2.3. *(i) If $\alpha = \beta = 0$, system (2.2) has a unique equilibrium $C(0,0)$ on $z = 0$. Moreover, the local dynamics of C is shown in Figure 4.*

(ii) If $\alpha > 0$ and $\beta = 0$, system (2.2) has two equilibria $E(\alpha, 0)$ and $C(0,0)$ on $z = 0$, where C is a saddle and E is a saddle.

(iii) If $\alpha = 0$ and $\beta > 0$, system (2.2) has two equilibria $F(1/\beta, 0)$ and $C(0,0)$ on $z = 0$, where F is a node and the local dynamics of C is shown in Figure 4.

(iv) If $\alpha > 0$ and $\beta > 0$, then

- *system (2.2) has a unique equilibrium $C(0,0)$ on $z = 0$ for $\alpha\beta > 1/4$, which is a saddle;*
- *system (2.2) has three equilibria $A\big(\frac{1+\sqrt{1-4\alpha\beta}}{2\beta}, 0\big)$, $B\big(\frac{1-\sqrt{1-4\alpha\beta}}{2\beta}, 0\big)$ and $C(0,0)$ on $z = 0$ for $\alpha\beta < 1/4$, where A and C are saddles, B is a node;*
- *system (2.2) has two equilibria $G(1/2\beta, 0)$ and $C(0,0)$ on $z = 0$ for $\alpha\beta = 1/4$. Moreover, C is a saddle and the local dynamics of G is shown in Figure 3.*

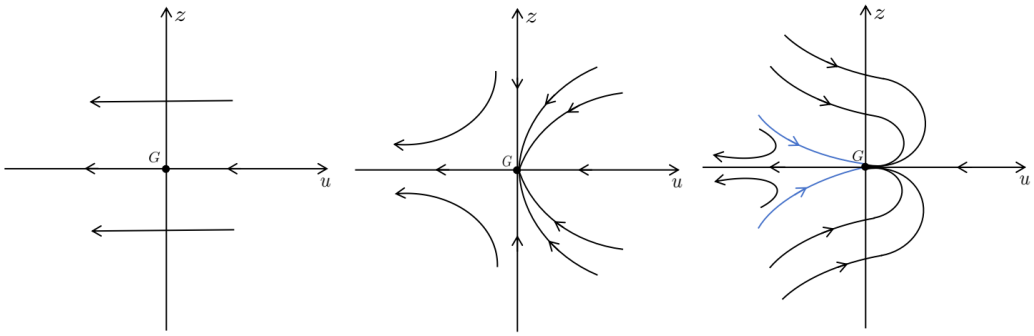

(a) $a > -(4\beta^2+1)/2\beta$ (b) $a = -(4\beta^2+1)/2\beta$ (c) $a < -(4\beta^2+1)/2\beta$

FIGURE 3. Local phase portraits of system (2.2) with $\alpha\beta = 1/4$ near G.

Proof. The equilibria of system (2.2) on $z = 0$ directly depend on the roots of $u(\beta u^2 - u + \alpha) = 0$. Thus, the number and locations of the equilibria of system (2.2) are clearly obtained.

(i) $\alpha = \beta = 0$. Taking the polar coordinate $(u, z) = (r\cos\theta, r\sin\theta)$, system (2.2) can be written as

$$\frac{1}{r}\frac{dr}{d\theta} = \frac{H_1(\theta) + \mathscr{O}(r)}{G_1(\theta) + \mathscr{O}(r)},$$

where

$$G_1(\theta) = \sin\theta(-\cos^2\theta + \sin^2\theta), \quad H_1(\theta) = -\cos\theta(-\cos^2\theta + \sin^2\theta).$$

According to [21, pp. 60], the exceptional directions of system (2.2) are determined by the zeros of $G_1(\theta)$. It is clear that $G_1(\theta)$ has six zeros $\theta = 0$, $\pi/4$, $3\pi/4$, π, $5\pi/4$, $7\pi/4$ in $[0, 2\pi)$. Moreover, $G_1'(0)H_1(0) = G_1'(\pi)H_1(\pi) = -1 < 0$, there is a unique orbit of system (2.2) approaching the origin along the directions $\theta = 0$ and π, respectively. However, for the other four directions, $H_1(\theta) = 0$. By using the blow-up $z = z_1 u$, system (2.2) is changed into

$$\begin{aligned} \frac{du}{d\eta} &= -z_1^2 u(u^2 + au + 1) + u, \\ \frac{dz_1}{d\eta} &= z_1^3(au + 1) - z_1, \end{aligned} \tag{2.4}$$

where $d\eta = u d\tau$. System (2.4) has three equilibria $O(0,0)$, $H^{\pm}(0, \pm 1)$ on $u = 0$. Furthermore, $(0,0)$ is a saddle, while the other two equilibria are semi-degenerate. By $(u, z_1) \mapsto (u, (z_1 - au)/2 + 1)$, system (2.4) reduces to

$$\begin{aligned} \frac{du}{d\eta} &= -\Big(\frac{z_1 - au}{2} + 1\Big)^2 u(u^2 + au + 1) + u, \\ \frac{dz_1}{d\eta} &= 2\Big(\frac{z_1 - au}{2} + 1\Big)^3 (au + 1) - 2\Big(\frac{z_1 - au}{2} + 1\Big) \\ &\quad + a\Big(-\Big(\frac{z_1 - au}{2} + 1\Big)^2 u(u^2 + au + 1) + u\Big). \end{aligned} \tag{2.5}$$

By the implicit function theorem, $dz_1/d\eta = 0$ has a unique root $z_1 = \phi_1(u)$ for small $|u|$. It follows from (2.5) that

$$\begin{aligned} &2\Big(\frac{z_1 - au}{2} + 1\Big)\frac{du}{d\eta} + u\frac{dz_1}{d\eta} \\ &= -2\Big(\frac{z_1 - au}{2} + 1\Big)^3 u^3 + au\Big(-\Big(\frac{z_1 - au}{2} + 1\Big)^2 u(u^2 + au + 1) + u\Big). \end{aligned}$$

Thus,

$$\frac{du}{d\eta}\Big|_{z_1 = \phi_1(u)} = -u^3 + o(u^3).$$

Finally, according to [21, Theorem 7.1 of Chapter 2], the origin of system (2.5) is a saddle. So is H^+ of system (2.4). Similarly, H^- of system (2.4) is also a saddle. Local dynamics of system (2.4) is depicted in Figure 4(a) and blowing down $H^{\pm}$ and O of system (2.4), we can obtain Figure 4(b).

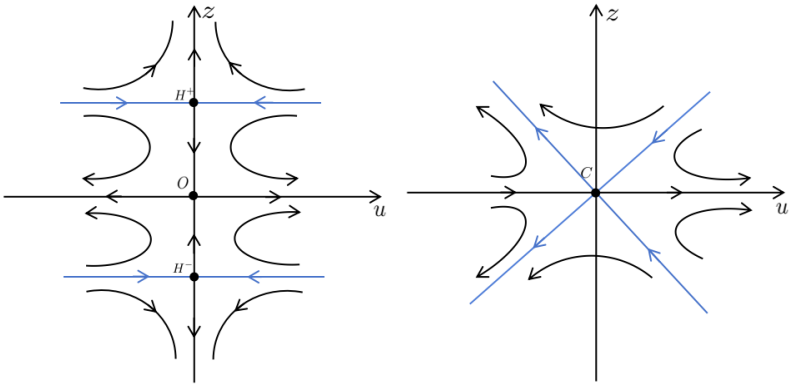

(a) Local dynamics of (2.4) (b) Local phase portrait of (2.2) near C

FIGURE 4. $\alpha = \beta = 0$ (or $\alpha = 0$ and $\beta > 0$).

(ii) $\alpha > 0$, $\beta = 0$. The Jacobian matrices at C and E are

$$J_C = \begin{pmatrix} -\alpha & 0 \\ 0 & 0 \end{pmatrix}, \quad J_E = \begin{pmatrix} \alpha & 0 \\ 0 & 0 \end{pmatrix},$$

implying that E and C are semi-degenerate. By the implicit function theorem, for system (2.2) $du/d\tau = 0$ has a unique root $u = \phi_2(z) = -z^2 + o(z^2)$ for small $|z|$. Thus,

$$\frac{dz}{d\eta}\Big|_{u=\phi_2(z)} = z^5 + o(z^5).$$

According to [21, Theorem 7.1 of Chapter 2], C is a saddle. Similarly, E is a saddle.

(iii) $\alpha = 0$, $\beta > 0$. In a manner analogous to (ii), we can obtain that F is a node. As for C, as studied in (i), we can get the results.

(iv) $\alpha > 0$, $\beta > 0$. As proved in (ii), C is a saddle of system (2.2). Consider $\alpha\beta < 1/4$. Let $u^* := (1+\sqrt{1-4\alpha\beta})/2\beta$. By the transformation $(u, z) \mapsto (u+u^*, z)$, system (2.2) is changed into

$$\begin{aligned} \frac{du}{d\tau} &= -z^2\left(u^2 + (a+2u^*)u + u^{*2} + au^* + 1\right) - \beta u^3 \\ &\quad - (3\beta u^* - 1)u^2 - (3\beta u^{*2} - 2u^* + \alpha)u, \\ \frac{dz}{d\tau} &= -u^* z^3 - z^3 u. \end{aligned} \tag{2.6}$$

According to [21, Theorem 7.1 of Chapter 2], the origin of system (2.6) is a saddle. So is A for system (2.2). Similarly, B is a node.

Consider $\alpha\beta = 1/4$. Let $u^* = 1/2\beta$. Then system (2.6) becomes

$$\begin{aligned} \frac{du}{d\tau} &= -z^2\Big(u^2 + \frac{a\beta+1}{\beta}u + \frac{1+2a\beta+4\beta^2}{4\beta^2}\Big) - \beta u^3 - \frac{1}{2}u^2, \\ \frac{dz}{d\tau} &= -\frac{1}{2\beta}z^3 - z^3 u. \end{aligned} \tag{2.7}$$

With the polar coordinates $(u, z) = (r\cos\theta, r\sin\theta)$, system (2.7) is transformed into

$$\frac{1}{r}\frac{dr}{d\theta} = \frac{H_2(\theta) + \mathscr{O}(r)}{G_2(\theta) + \mathscr{O}(r)},$$

where

$$G_2(\theta) = \sin\theta\Big(\frac{1}{2}\cos^2\theta + \frac{1+2a\beta+4\beta^2}{4\beta^2}\sin^2\theta\Big),$$
$$H_2(\theta) = -\cos\theta\Big(\frac{1}{2}\cos^2\theta + \frac{1+2a\beta+4\beta^2}{4\beta^2}\sin^2\theta\Big).$$

The zeros of $G_2(\theta)$ are strongly related to the sign of $-(1+2a\beta+4\beta^2)$.

Firstly, if $-(1+2a\beta+4\beta^2) < 0$ (i.e. $a < (4\beta^2+1)/2\beta$), $G_2(\theta) = 0$ has two roots $\theta = 0$, π in $\theta \in [0, 2\pi)$. It is clear that $G_2'(0)H_2(0) = G_2'(\pi)H_2(\pi) = -1/4 < 0$. By [21, Theorem 3.7 of Chapter 2], there is a unique orbit of system (2.2) approaching the origin along the directions $\theta = 0$ and π, respectively. The local phase portrait of system (2.2) near the origin is shown in Figure 3(a).

Secondly, if $1+2a\beta+4\beta^2 = 0$ (i.e. $a = -(1+4\beta^2)/2\beta$), $G_2(\theta) = 0$ has four roots $\theta = 0$, $\pi/2$, π, $3\pi/2$ in $\theta \in [0, 2\pi)$. A direct calculation gives $G_2'(0)H_2(0) = G_2'(\pi)H_2(\pi) = -1/4 < 0$. By [21, Theorem 3.7 of Chapter 2], there is a unique orbit of system (2.2) approaching the origin along the directions $\theta = 0$ and π, respectively. To study the other two directions, the change of variables $u = u_1 z$ is applied, by which system (2.7) is transformed into

$$\begin{aligned} \frac{du_1}{d\eta} &= -\frac{2a\beta+1}{2\beta}u_1 z - \beta u_1^3 z - \frac{1}{2}u_1^2, \\ \frac{dz}{d\eta} &= -\frac{1}{2\beta}z^2 - z^3 u_1, \end{aligned} \tag{2.8}$$

where $d\eta = z d\tau$. With the polar coordinates $(u, z) = (r\cos\theta, r\sin\theta)$, system (2.8) becomes

$$\frac{1}{r}\frac{dr}{d\theta} = \frac{H_3(\theta) + \mathscr{O}(r)}{G_3(\theta) + \mathscr{O}(r)},$$

where

$$G_3(\theta) = \sin\theta\cos\theta\Big(a\sin\theta + \frac{1}{2}\cos\theta\Big),$$
$$H_3(\theta) = -\frac{1}{2\beta}\sin^3\theta - \frac{2a\beta+1}{2\beta}\cos^2\theta\sin\theta - \frac{1}{2}\cos^3\theta.$$

Hence, $G_3(\theta) = 0$ has four roots $\theta = 0$, $\arctan(\beta/(1+4\beta^2))$, $\pi/2$, π, $\pi + \arctan(\beta/(1+4\beta^2))$, $3\pi/2$ in $\theta \in [0, 2\pi)$. Moreover,

$$G_3'(0)H_3(0) = G_3'(\pi)H_3(\pi) = -\frac{1}{4} < 0,$$
$$G_3'(\pi/2)H_3(\pi/2) = G_3'(3\pi/2)H_3(3\pi/2) = -\frac{1+4\beta^2}{4\beta^2} < 0,$$
$$\begin{aligned} &G_3'\Big(\arctan\big(\frac{\beta}{1+4\beta^2}\big)\Big)H_3\Big(\arctan\big(\frac{\beta}{1+4\beta^2}\big)\Big) \\ &= G_3'\Big(\pi + \arctan\big(\frac{\beta}{1+4\beta^2}\big)\Big)H_3\Big(\pi + \arctan\big(\frac{\beta}{1+4\beta^2}\big)\Big) \\ &= \frac{(4a^2+1)^2}{64a^4(1+4\beta^2)}\cos^6\Big(\arctan\big(\frac{\beta}{1+4\beta^2}\big)\Big) > 0. \end{aligned}$$

By [21, Theorems 3.7 and 3.8 of Chapter 2], we can obtain that for system (2.8) there are infinitely many orbits approaching the origin in respectively the directions $\arctan(\beta/(1+4\beta^2))$, $\pi + \arctan(\beta/(1+4\beta^2))$, a unique orbit approaching the origin in respectively the directions 0, $\pi/2$, π, $3\pi/2$. Performing the blow-down of the point O in system (2.8) then leads to the phase portrait depicted in Figure 3(b).

Thirdly, if $-(1+2a\beta+4\beta^2)>0$ (i.e. $a>(4\beta^2+1)/2\beta$), we consider $z=uz_1$, then system (2.7) is changed into

$$\begin{aligned}\frac{du}{d\xi}&=-uz_1^2\Big(u^2+\frac{a\beta+1}{\beta}u+\frac{1+2a\beta+4\beta^2}{4\beta^2}\Big)-\beta u^2-\frac{1}{2}u,\\ \frac{dz_1}{d\xi}&=\frac{2a\beta+1}{2\beta}z_1^3u+\beta uz_1+\frac{1+2a\beta+4\beta^2}{4\beta^2}z_1^3+\frac{1}{2}z_1,\end{aligned}\tag{2.9}$$

where $d\xi=ud\tau$. System (2.9) has three equilibria, denoted by $H^{\pm}\,(0,\pm z_1^*)$ and $O(0,0)$ on $u=0$, where $z_1^*=\sqrt{-2\beta^2/(1+2a\beta+4\beta^2)}$. In addition, O is a saddle and $H^{\pm}$ are semi-degenerate. By considering $z_1\mapsto z_1+z_1^*$, system (2.9) reduced to

$$\begin{aligned}\frac{du}{d\xi}&=-u(z_1+z_1^*)^2\Big(u^2+\frac{a\beta+1}{\beta}u+\frac{1+2a\beta+4\beta^2}{4\beta^2}\Big)-\beta u^2-\frac{1}{2}u,\\ \frac{dz_1}{d\xi}&=\frac{2a\beta+1}{2\beta}(z_1+z_1^*)^3u+\beta u(z_1+z_1^*)+\frac{1+2a\beta+4\beta^2}{4\beta^2}(z_1+z_1^*)^3+\frac{1}{2}(z_1+z_1^*).\end{aligned}\tag{2.10}$$

From (2.10), we have

$$(z_1+z_1^*)\frac{du}{d\xi}+u\frac{dz_1}{d\xi}=-\frac{1}{2\beta}u^2(z_1+z_1^*)^3-u^3(z_1+z_1^*)^3.$$

Thus,

$$\frac{du}{d\xi}=-\frac{1}{2\beta}z_1^{*2}u^2+o(u^2)$$

when $dz_1/d\xi=0$. According to [21, Theorem 7.1 of Chapter 2], the origin of system (2.10) is a saddle-node. So is H^+ for system (2.9). Similarly, H^- is also a saddle-node, see Figure 5. Further, Figure 3(c) is obtained. □

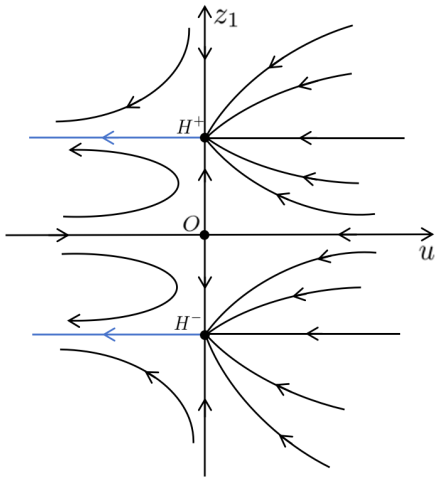

FIGURE 5. Local phase portrait of (2.9) with $\alpha\beta=1/4$ and $-(1+2a\beta+4\beta^2)>0$.

Lemma 2.4. *For system* (2.3), $D(0,0)$ *is an unstable star node for* $\beta>0$, *and a degenerate equilibrium for* $\beta=0$. *Moreover, the qualitative properties of* D *for* $\beta=0$ *is shown in Figure 6.*

Proof. Firstly, we can obtain D is an unstable star node due to the Jacobian matrix of system (2.3) at D when $\beta>0$. Secondly, for $\beta=0$, by the polar coordinate $(v,z)=(r\cos\theta,r\sin\theta)$, system (2.3) is transformed into

$$\frac{1}{r}\frac{dr}{d\theta}=\frac{H_4(\theta)+\mathscr{O}(r)}{G_4(\theta)+\mathscr{O}(r)},$$

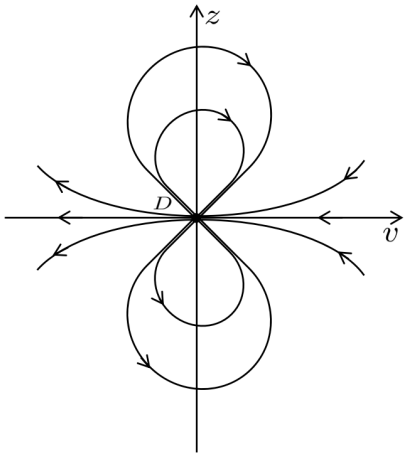

FIGURE 6. Local phase portrait of system (2.3) near $D(0,0)$.

where

$$G_4(\theta) = -\sin^3\theta, \quad H_4(\theta) = \cos^3\theta.$$

Further, $\theta = 0, \pi$ are zeros of three-multiple of $G_4(\theta)$. One can check $G_4'''(0)H_4(0) = G_4'''(\pi)H_4(\pi) = 6$. By [21, Theorems 3.7 and 3.8 of Chapter 2], system (2.3) has infinitely many orbits approaching D in the directions $\theta = 0, \pi$. Consequently, the qualitative properties of D for $\beta = 0$ is shown in Figure 6. □

From Lemmas 2.3 and 2.4, we can summarize the dynamics of the equilibria at infinite in the Poincaré disc for system (1.3) as follows.

Proposition 2.5. *All phase portraits in the Poincaré disc of system* (1.3) *near infinity can be classified in Figure 7. Here,* $I_A^{\pm}$, $I_B^{\pm}$, $I_C^{\pm}$, $I_D^{\pm}$, $I_E^{\pm}$, $I_F^{\pm}$, $I_G^{\pm}$ *are equilibria at infinity of system* (1.3), *which correspond to those equilibria of systems* (2.2) *and* (2.3), *respectively.*

3. Limit cycles of system (1.3)

In this section, we establish several sufficient and necessary conditions for the existence of limit cycles in system (1.3). We begin by presenting two preliminary lemmas concerning the nonexistence and uniqueness of limit cycles in planar dynamical systems respectively.

Lemma 3.1 ([6, Theorem 1])**.** *Consider the system*

$$\dot{x} = y, \quad \dot{y} = -g(x) - f(x,y)y, \tag{3.1}$$

where $x \in (\alpha, \beta)$, $y \in \mathbb{R}$, $\alpha < 0$, $\beta > 0$. *Assume that* $g(x) = -g(-x)$ *for all* $0 \leqslant x < \min\{-\alpha, \beta\}$, *and that the following conditions hold:*

(i) $xg(x) > 0$ *for all* $(\alpha, 0) \cup (0, \beta)$;
(ii) $g(x)$ *is Lipschitzian continuous for* $x \in (\alpha, 0) \cup (0, \beta)$, *and* $f(x,y)$ *is Lipschitzian continuous for* $(x,y) \in (\alpha, \beta) \times \mathbb{R}$;
(iii) *either* $f(x,y) \geqslant -f(-x,y)$ *or* $f(x,y) \leqslant -f(-x,y)$ *for all* $0 \leqslant x < \min\{-\alpha, \beta\}$ *and* $y \in \mathbb{R}$;
(iv) $f(x,y) \not\equiv -f(-x,y)$ *for* $x \in (0, \zeta)$ *and* $y \in \mathbb{R}$, *where* $0 < \zeta \ll 1$.

Then, system (3.1) *has no closed orbits in the strip* $\alpha < x < \beta$.

Lemma 3.2 ([5, Theorem 1])**.** *Consider the system*

$$\dot{x} = y, \quad \dot{y} = -|x|^m \operatorname{sgn}(x) - f(x,y)y, \tag{3.2}$$

where $1 \leq m < +\infty$ *and* $f(x,y)$ *is continuous in* $\mathbb{R}^2$, *which satisfies the conditions that ensure the existence and uniqueness of solutions for the initial value problem of system* (3.2).

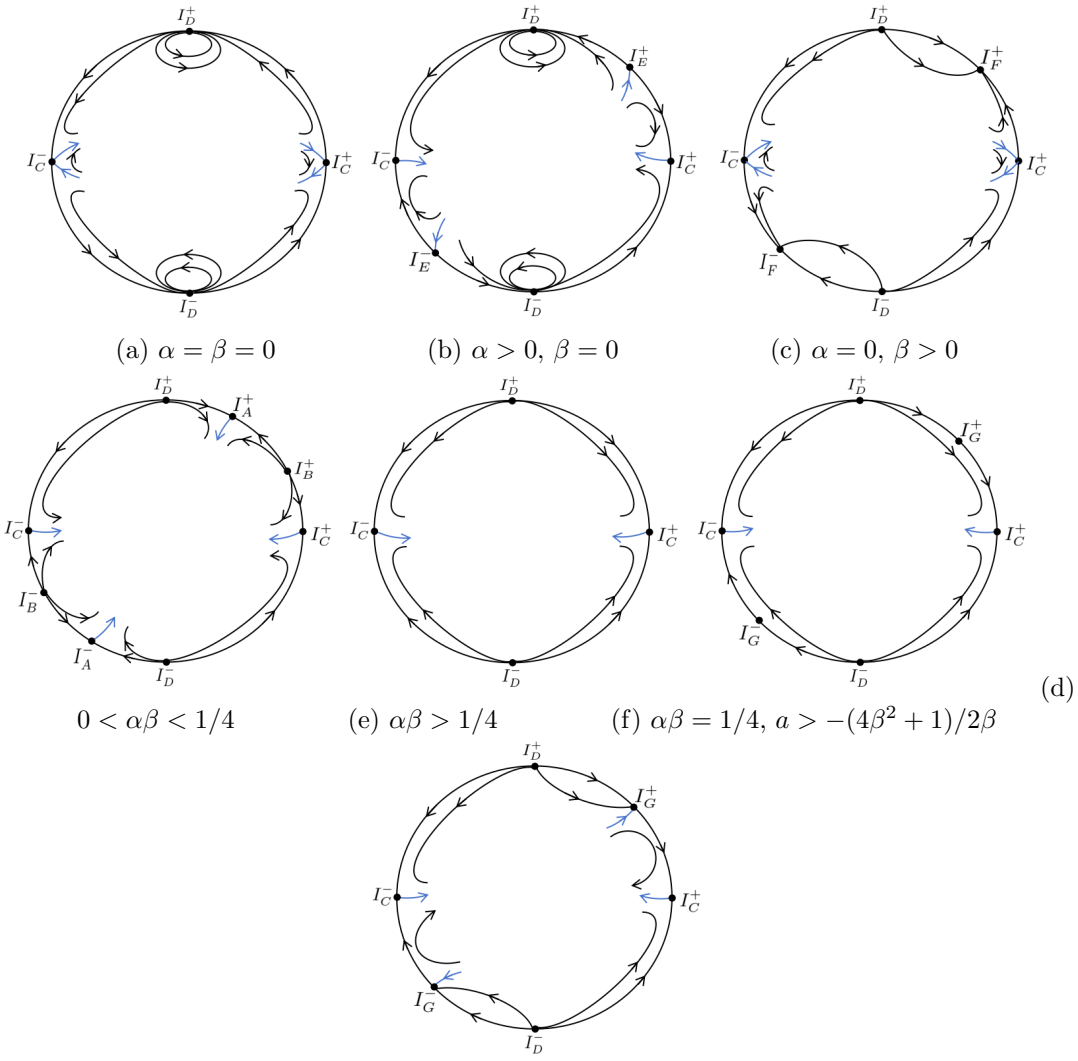

(a) $\alpha = \beta = 0$ (b) $\alpha > 0$, $\beta = 0$ (c) $\alpha = 0$, $\beta > 0$

$0 < \alpha\beta < 1/4$ (e) $\alpha\beta > 1/4$ (f) $\alpha\beta = 1/4$, $a > -(4\beta^2+1)/2\beta$ (d)

(g) $\alpha\beta = 1/4$, $a \le -(4\beta^2+1)/2\beta$

FIGURE 7. Equilibria at infinity of system (1.3) in the Poincaré disc.

If for all small ε and k with $0 < k < 1$, $f(x,y)$ satisfies

$$k^{(1-m)/2} f(kx, k^{(1+m)/2} y) \le f(x,y), \quad \forall x, y \in \mathbb{R},$$
$$k^{(1-m)/2} f(kx, k^{(1+m)/2} y) \ne f(x,y) \quad \text{for } x \ne 0,\ 0 < |y| < \varepsilon,$$

then system (3.2) *has at most one limit cycle. Moreover, the limit cycle is stable if it exists.*

Proposition 3.3. *There are no closed orbits of system* (1.3) *when either $a \ge 0, \alpha^2 + \beta^2 \ne 0$ or $a \ne 0, \alpha = \beta = 0$.*

Proof. Set $g(x) = x$ and $f(x,y) = a + \alpha x^2 - xy + \beta y^2$. Obviously, $g(x)$ is an odd function. One can check that the conditions (i) and (ii) of Lemma 3.1 hold for $(x,y) \in \mathbb{R}^2$. Also, $f(x,y) + f(-x,y) = 2a + 2\alpha x^2 + 2\beta y^2 \ge 0$ holds for $a \ge 0$. Then the condition (iii) of Lemma 3.1 holds, and so does the condition (iv), because $\alpha^2 + \beta^2 \ne 0$. By Lemma 3.1, system (1.3) has no closed orbits around the origin when $a \ge 0$ and $\alpha^2 + \beta^2 \ne 0$. Similarly, we can obtain that there are no closed orbits for system (1.3) when $\alpha = \beta = 0$ and $a \ne 0$. □

From [5, Theorem 13], we can derive the following result immediately.

Proposition 3.4. *There is a unique limit cycle of system* (1.3) *when* $a < 0$ *and* $\alpha\beta \geq 1/4$.

Next, we state two lemmas, which are concerned with the limit cycles of system (1.3) for the case $a < 0$ and $\alpha\beta = 0$. The idea for their proofs goes back to Levinson and Smith [14].

Lemma 3.5. *When* $a < 0$, $\alpha = 0$ *and* $\beta > 0$, *we have*

(i) *system* (1.3) *has no limit cycles for* $a + \beta \leq 0$;
(ii) *system* (1.3) *has one limit cycle for* $a + \beta > 0$.

Proof. For system (1.3), we calculate

$$\frac{dy}{dt}\big|_{y=1} = -a - \beta, \quad \frac{dy}{dt}\big|_{y=-1} = a + \beta. \tag{3.3}$$

Thus, if system (1.3) has any limit cycles, they must be in the strip $|y| < 1$. Using the time-scaling

$$dt \mapsto -\frac{1}{1-y^2}dt,$$

we re-write (1.3) as

$$\begin{aligned} \frac{dx}{dt} &= -\frac{y}{1-y^2} =: -g(y), \\ \frac{dy}{dt} &= x + \frac{ay + \beta y^3}{1-y^2} =: x - F(y). \end{aligned} \tag{3.4}$$

We claim that systems (1.3) and (3.4) are topologically equivalent in the strip $|y| < 1$. Hence, we can obtain that systems (1.3) and (3.4) have the same number of limit cycles. In conclusion, to study the number of limit cycles of system (1.3), it suffices to consider the corresponding problem for system (3.4), a Liénard form.

When system (3.4) satisfies $a + \beta \leq 0$, the divergence is

$$\operatorname{div}(-g(y), x - F(y)) = -\beta + \frac{(a+\beta)(1+y^2)}{(1-y^2)^2} < 0.$$

Thus, statement (i) holds.

Consider system (3.4) with $a + \beta > 0$. The energy function is

$$\mathcal{E}(x, y) = \frac{x^2}{2} + \int_0^y \frac{s}{1-s^2}ds. \tag{3.5}$$

We can check that the function $x = F(y)$ has the following properties. $F(y)$ is strictly decreasing on the interval $(-\Delta, \Delta)$ and strictly increasing on the intervals$(-1, -\Delta)$ and $(\Delta, 1)$, where

$$\Delta = \sqrt{\frac{(3\beta + a) + \sqrt{(3\beta + a)^2 + 4a\beta}}{2\beta}}.$$

Furthermore, $F(y) < 0$ for $y \in (-1, -\sqrt{-a/\beta}) \cup (0, \sqrt{-a/\beta})$, while $F(y) > 0$ for $y \in (-\sqrt{-a/\beta}, 0) \cup (\sqrt{-a/\beta}, 1)$. The graph of $x = F(y)$ is shown in Figure 8.

Assume that system (3.4) with $a + \beta > 0$ has at least two limit cycles. Let Γ_1 and Γ_2 denote the two limit cycles closest to the equilibrium O with Γ_2 enclosing Γ_1. We now claim that points $\big(0, \pm\sqrt{-a/\beta}\big)$ are in the region enclosed by Γ_1. In fact, if Γ_1 is in the strip $|y| < \sqrt{-a/\beta}$, $d\mathcal{E}/dt < 0$ for $|y| < \sqrt{-a/\beta}$ and $\mathcal{E}(x, y)$ is defined by (3.5). This leads a contradiction to the existence of a limit cycle. For $i = 1, 2$, let A_i and D_i denote the intersection points of Γ_i with the line $y = 0$, where A_i (resp. D_i) lie on the positive (resp. negative) x-axis. Let B_i and C_i denote the intersection points of Γ_i with the line $y = \sqrt{-a/\beta}$, where B_i (resp. C_i) lie in the first quadrant (resp. the second quadrant). Let E_2 and F_2 be two points on the curve Γ_2, located vertically above the line $y = \sqrt{-a/\beta}$, and having the same abscissas as B_1 and C_1, denoted by x_{B_1} and x_{C_1}, respectively.

The equal sign in the energy function $\mathcal{E}(x, y)$ gives

$$\oint_{\Gamma_i} d\mathcal{E} = \oint_{\Gamma_i} F(y)dx = 0, \quad i = 1, 2.$$

Since the vector field of (3.4) is symmetric with respect to the origin, it leads to

$$0 = \oint_{\Gamma_i} F(y)dx = 2\int_{\widehat{A_iD_i}} F(y)dx, \ \ i = 1, 2. \tag{3.6}$$

By calculation, we have

$$\begin{aligned}
&\int_{\widehat{A_1B_1}} F(y)dx - \int_{\widehat{A_2B_2}} F(y)dx \\
&= \int_0^{\sqrt{-a/\beta}} \frac{-g(y)F(y)}{x_1(y) - F(y)}dy - \int_0^{\sqrt{-a/\beta}} \frac{-g(y)F(y)}{x_2(y) - F(y)}dy \\
&= \int_0^{\sqrt{-a/\beta}} \frac{-g(y)F(y)\left(x_2(y) - x_1(y)\right)}{(x_1(y) - F(y))(x_2(y) - F(y))}dx,
\end{aligned}$$

where $x = x_1(y)$ and $x = x_2(y)$ stand for the curves $\widehat{A_1B_1}$ and $\widehat{A_2B_2}$ respectively with $y \in (0, \sqrt{-a/\beta})$. Since $x_2(y) > x_1(y) > 0 > F(y)$ and $g(y) > 0$ for $y \in (0, \sqrt{-a/\beta})$, we have that

$$\int_{\widehat{A_1B_1}} F(y)dy > \int_{\widehat{A_2B_2}} F(y)dx. \tag{3.7}$$

Similarly, we have

$$\int_{\widehat{C_1D_1}} F(y)dy > \int_{\widehat{C_2D_2}} F(y)dy. \tag{3.8}$$

Let $y = y_1(x)$ and $y = y_2(x)$ stand for the curves $\widehat{B_1C_1}$ and $\widehat{E_2F_2}$ respectively with $x \in (x_{C_1}, x_{B_1})$. Then

$$\int_{\widehat{B_1C_1}} F(y)dx - \int_{\widehat{E_2F_2}} F(y)dx = \int_{x_{B_1}}^{x_{C_1}} \left(F(y_1(x)) - F(y_2(x))\right)dx > 0. \tag{3.9}$$

Since $F(y) > 0$ on curves $\widehat{B_2E_2}$ and $\widehat{F_2C_2}$,

$$\int_{\widehat{B_2E_2}\cup\widehat{F_2C_2}} F(y)dx < 0. \tag{3.10}$$

From (3.7)-(3.10), it follows that

$$\int_{\widehat{A_1D_1}} F(x)dy > \int_{\widehat{A_2D_2}} F(x)dy,$$

which contradicts (3.6). In other words, system (3.4) with $a + \beta > 0$ has at most one limit cycle, so is system (1.3). Further, on the one hand, according to Lemma 2.1, the unique equilibrium O of system (1.3) is a source. On the other hand, from (3.3), we have $dy/dt < 0$ on the line $y = 1$ and $dy/dt > 0$ on the line $y = -1$. Therefore, we take the point O as the inner boundary and the lines $y = \pm 1$ as the outer boundary. By applying the Poincaré-Bendixson Theorem in the annular region defined by $|y| < 1$, it follows that system (1.3) admits at least one limit cycle within this strip. In summary, when $a < 0$ with $a + \beta > 0$, system (1.3) has exactly one limit cycle. This completes the proof of statement (ii). □

Lemma 3.6. *When $a < 0$, $\alpha > 0$ and $\beta = 0$, we have that* (i) *system* (1.3) *has no limit cycles for $a + \alpha \le 0$; and* (ii) *system* (1.3) *has one limit cycle for $a + \alpha > 0$.*

Proof. Making the transformation

$$(x, y, dt) \mapsto \Big(x, y\exp\big(\frac{1}{2}x^2\big), \exp\big(-\frac{1}{2}x^2\big)dt\Big),$$

we re-write (1.3) as

$$\begin{aligned}
\frac{dx}{dt} &= y, \\
\frac{dy}{dt} &= -x\exp(-x^2) - (a + \alpha x^2)\exp\big(\frac{-x^2}{2}\big)y =: -g(x) - f(x)y.
\end{aligned} \tag{3.11}$$

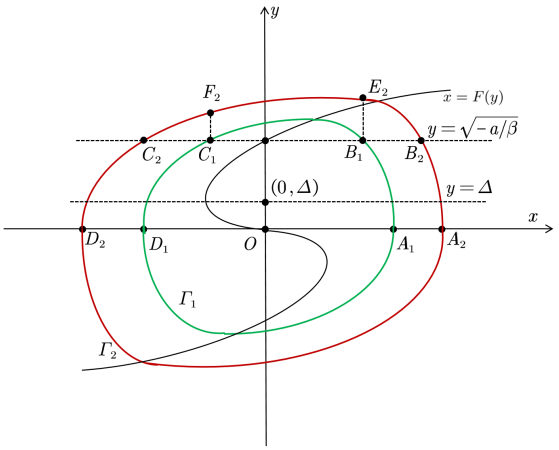

FIGURE 8. The uniqueness of limit cycle of system (3.4) with $a + \beta > 0$.

Making the transformation

$$y \mapsto y - \int_0^x f(s)ds =: y - F(x),$$

we convert (3.11) to the equivalent system

$$\begin{aligned} \frac{dx}{dt} &= y - \int_0^x \Big((a + \alpha s^2)\exp\big(\frac{-s^2}{2}\big)\Big)ds = y - F(x), \\ \frac{dy}{dt} &= -x\exp\big(-x^2\big) = -g(x). \end{aligned} \tag{3.12}$$

We can obtain that the number of limit cycles in system (1.3) is equal to that in system (3.12). Therefore, instead of analyzing system (1.3) directly, we can study the limit cycles of system (3.12). For system (3.12), the analysis is nearly identical to that in Lemma 3.5, and thus the details are omitted here. □

We remark that some of the assumptions stated by Levinson and Smith do not hold in our setting. For systems (3.4) and (3.12), $\int_0^\infty f(x)\,dx = \int_0^\infty g(x)\,dx = +\infty$ does not hold, so the Levinson-Smith argument cannot be applied directly. In fact, the condition is specifically used to prove the existence of limit cycles. If we are only concerned with the uniqueness of limit cycles, this condition is not sufficient.

4. Proof of Theorem 1.1

According to Lemma 2.1 and Proposition 2.5, we can obtain the number and position of equilibria of system (1.3) at finite points and infinity. For any given $\alpha = \alpha^*$, the equilibria of system (2.2) on $z = 0$ directly depend on the roots of $u(\beta u^2 - u + \alpha) = 0$ by Lemma 2.3. Thus, SN is a saddle-node bifurcation surface for the equilibria of system (1.3) at infinity. Consequently, we obtain Part (a). Further, we can obtain from Lemma 2.3 that C is a cusp bifurcation surface for the equilibria of system (1.3) at infinity and we arrive at Part (b). Part (c) follows from Lemma 2.2 immediately that H is a Hopf bifurcation surface.

For a given $\alpha = \alpha^*$, Lemma 3.6 implies that system (1.3) possesses a unique and stable limit cycle γ when $\beta = 0$ and $-\alpha^* < a < 0$. Referring to Figure 7(b), the α-limit set of the unstable manifold of I_E^+ is either I_C^- or I_D^+.

We now claim that the α-limit set is indeed I_D^+. Suppose, to the contrary, that the α-limit set of the unstable manifold of I_E^+ were I_C^- (as shown in Figure 9(a)). Since system (1.3) constitutes a generalized rotated vector field with respect to the parameter a (see [21, Section 3, Chapter 4]), a small perturbation $\alpha \mapsto \alpha - \varepsilon$ would cause the saddle connection to break, as illustrated in Figure 9(b). Under such a sufficiently small perturbation, the original stable limit cycle γ

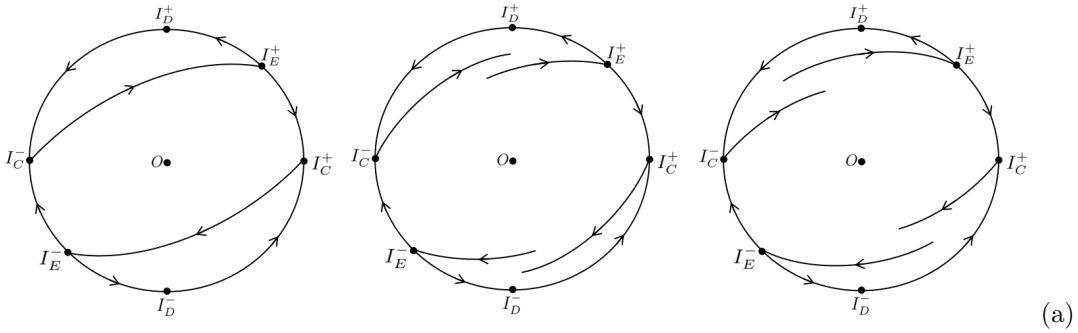

FIGURE 9. Manifolds of equilibria at infinity.

persists. However, by the Poincaré–Bendixson annular region theorem, the resulting phase portrait (Figure 9(b)) would imply the emergence of a new limit cycle enclosing γ, leading to a contradiction with the uniqueness of limit cycles. Therefore, the claim is valid. Consequently, we obtain the global phase portrait for the case $\alpha = \alpha^*$, $\beta = 0$, and $-\alpha^* < a < 0$, depicted in Figure 2(b).

A direct computation shows that the line $y = \alpha^* x$ is invariant for $\beta = 0$ and $a = -\alpha^* - 1/\alpha^* < -\alpha^*$, meaning that the α-limit set of the unstable manifold of I_E^+ is O. Since $\beta = 0$ and $-\alpha^* < a < 0$, we have that the α-limit set of the unstable manifold of I_E^+ is I_D^+. Based on the theory of rotated vector fields, for $\beta = 0$, there exists a value $a = a_0$ with $a_0 \in (-\alpha^* - 1/\alpha^*, -\alpha^*]$ such that the α-limit set of the unstable manifold of I_E^+ is I_C^-. We now show that $a_0 = -\alpha^*$. If $a = a_0 < -\alpha^*$, for system (1.3), there are no limit cycles and the the saddle connection between I_E^+ and I_C^-. Moreover, since the saddle connection is structurally unstable, then the saddle connection will rupture and the relative location of the manifolds of I_E^+ and I_C^- is shown as Figure 9(c) when taking the perturbation $a_0 \mapsto a_0 + \varepsilon$ such that $a_0 + \varepsilon < \alpha^*$. Similarly, according to the Poincaré-Bendixson annular region theorem, there will lead a limit cycle get a contradiction. Thus, $a_0 = -\alpha^*$. Finally, the global phase portraits Figure 2(c) and Figure 2(d), which correspond to the cases with $\beta = 0$, $a = -\alpha^*$ and $\beta = 0$, $a < -\alpha^*$ respectively, can be readily determined. In summary, S is a generalized heteroclinic bifurcation surface, so is HL. This completes the proof of Parts (d), (e).

For the global phase portraits of system (1.3), due to the symmetry of its vector fields with respect to the origin, it suffices to consider $y \geq 0$. When $(\alpha, \beta, a) \in L_2$ (or S, L_3, VI, HL, VII), the results from the previous proofs allow us to complete the global phase portrait; see Figure 2(b) (or c, d, o, p, q). By combining the local dynamics near equilibria (see Lemma 2.1) with the behavior at infinity (see Proposition 2.5) and the results on limit cycles (see Propositions 3.3, 3.4, and 3.5), we directly obtain the global phase portraits for $(\alpha, \beta, a) \in L_1$ (or I, III, IV, SN_1, SN_2, $SN_3 \cup C$, V); see Figure 2(a) (or e, f, g, h, i, j, k).

Next, we consider the cases $(\alpha, \beta, a) \in O$ (or L_4, L_5). When $(\alpha, \beta, a) \in O$, Lemma 2.1 shows that O is a center, and the vector fields of system (1.3) are symmetric with respect to both the x-axes and y-axes. This symmetry immediately yields the global phase portrait shown in Figure 2(m).

For $(\alpha, \beta, a) \in L_4$, the connection between I_C^- and I_C^+ is structurally unstable. Thus, the ω-limit set of the unstable manifold of I_C^- must be either O or I_D^+. We claim that the ω-limit set is O. Suppose, for contradiction, that the ω-limit set is I_D^+. Since the origin O is a stable equilibrium, the Poincaré–Bendixson annular region theorem would then imply the existence of a limit cycle, contradicting Proposition 3.3. Hence, the claim is valid.

Referring to Figure 7(a), we obtain the global phase portrait for $\alpha = 0$, $\beta = 0$, and $a > 0$, depicted in Figure 2(l). By the same reasoning, the global phase portrait in Figure 2(n) is obtained.

5. Comparison and description

In this section, we provide a brief comparison of the global dynamics of systems (1.2) and (1.3), and we explain why the analysis of limit cycles for system (1.3) is more involved. Finally, we present a discussion of limit cycles of system (1.3) in the case $a < 0$ and $0 < \alpha\beta < 1/4$.

Comparison of the global dynamics of systems (1.2) **and** (1.3)**.** In general, the global bifurcation diagram of system (1.2) consists of a saddle-node bifurcation surface at infinity, a cusp bifurcation surface, and a Hopf bifurcation surface (see [3]). In contrast, the bifurcation structure of system (1.3) is richer: in addition to the same saddle-node, cusp, and Hopf bifurcations, system (1.3) exhibits two additional generalized heteroclinic bifurcation surfaces.

We analyze the systems in terms of equilibria and limit cycles to highlight both commonalities and differences. Firstly, systems (1.2) and (1.3) share the same types of equilibria at finite points, but differ in the equilibria at infinity. Secondly, when $\alpha\beta \neq 0$, both systems display consistent bifurcation phenomena and possess the same number of limit cycles. In particular, when $a < 0$, each system has a unique limit cycle; when $a \geq 0$, neither system has any limit cycles.

However, when $\alpha\beta = 0$, the bifurcation phenomena and the number of limit cycles differ between the two systems. System (1.2) has a unique limit cycle for $a < 0$ and none for $a \geq 0$. For system (1.3), there is similarly no closed orbit when $a \geq 0$. Moreover, a generalized heteroclinic bifurcation occurs in system (1.3) when $a + \alpha = 0$ (resp. $a + \beta = 0$) for $\beta = 0$ (resp. $\alpha = 0$). Consequently, for $a < 0$, system (1.3) has a unique limit cycle if $a + \alpha > 0$ (resp. $a + \beta > 0$) for $\beta = 0$ (resp. $\alpha = 0$), and no limit cycle if $a + \alpha \leq 0$ (resp. $a + \beta \leq 0$).

Discussion of limit cycles of system (1.3) **when** $a < 0$ **and** $0 < \alpha\beta < 1/4$**.** A natural question arises: since systems (1.2) and (1.3) are derived from the same underlying equation (1.1), why can the bifurcation diagram and all global phase portraits in the Poincaré disc for system (1.2) be fully resolved, while system (1.3) remains challenging to analyze? The main difficulty lies in determining the number of limit cycles when $a < 0$ and $0 < \alpha\beta < 1/4$. For system (1.2), comparing integrals along corresponding arcs suffices to establish the uniqueness of the limit cycle. However, in system (1.3), although the integral expression for the divergence is formally the same, the sign of the cross term xy differs from that of the x^2 and y^2 terms. This difference prevents a straightforward comparison of the divergence integral and makes it difficult to rigorously determine the number of limit cycles in this parameter regime.

It is worth noting that when $-\varepsilon < a < 0$ and $0 < \alpha\beta < 1/4$ with sufficiently small $\varepsilon > 0$, a subset of this parameter space yields a unique stable limit cycle. Indeed, by the classical Hopf bifurcation theorem (see Lemma 2.2), system (1.3) possesses a unique stable limit cycle Γ near the origin. We now show that no limit cycles exist outside a sufficiently small neighborhood of the origin. Assume, for contradiction, that there exists at least one limit cycle outside this neighborhood. Let γ denote the limit cycle closest to Γ. By stability of Γ, γ must be internally unstable, i.e.,

$$\oint_\gamma \left(a + \alpha x^2 + 3\beta y^2\right) ds \leq 0.$$

However, since a is sufficiently small and γ lies outside this neighborhood, we have

$$a + \alpha x^2 + 3\beta y^2 > 0 \quad \text{for } (x, y) \in \gamma,$$

which contradicts the inequality above. Therefore, no limit cycles exist outside the small neighborhood of the origin. Consequently, when $-\varepsilon < a < 0$ and $0 < \alpha\beta < 1/4$, system (1.3) has a unique stable limit cycle. Based on this observation, we propose the following conjecture.

Conjecture 5.1. When $a < 0$ and $0 < \alpha\beta < 1/4$, system (1.3) has exactly one limit cycle, which is stable and hyperbolic.

Acknowledgements. This work was supported by the National Natural Science Foundation of China (Nos. 12322109, 12571190), and by the Hunan Basic Science Research Center for Mathematical Analysis (2024JC2002). R. Zhang was supported by the Hunan Provincial Innovation Foundation for Postgraduates (No. CX20240165).

References

[1] J. F. Cariñena, M. F. Rañada, M. Santander, M. Senthilvelan; A non-linear oscillator with quasi-harmonic behaviour: two- and n- dimensional oscillators, *Nonlinearity*, **17** (2004), 1941-1963.

[2] H. Chen, Z. Feng, R. Zhang; Global phase portraits of separable polynomial rigid systems with a center, *J. Nonlinear Sci.*, **35** (1) (2025), Paper No. 6, 49 pp.

[3] H. Chen, K. Gebreselassie, Y. Lu, R. Zhang; Global dynamics of a modified hybrid Van der Pol-Rayleigh oscillator, *Acta Math. Sin. (Engl. Ser.)* to appear.

[4] H. Chen, Y. Tang, D. Xiao; Global dynamics of hybrid van der Pol-Rayleigh oscillators, *Phys. D*, **428** (2021), 133021.

[5] H. Chen, Y. Tang, D. Xiao; On the uniqueness of limit cycles in second-order oscillators, *J. Differential Equations*, **370** (2023), 140-166.

[6] H. Chen, H. Yang, R. Zhang, X. Zhang; New criterions on nonexistence of periodic orbits of planar dynamical systems and their applications, *J. Nonlinear Sci.*, **34** (2024), Paper No. 96, 66 pages.

[7] S. -N. Chow, C. Li, D. Wang; *Normal Forms and Bifurcation of Planar Vector Fields*, Cambridge University Press, NewYork, 1994.

[8] C. Christopher, D. Schlomiuk; On general algebraic mechanisms for producing centers in polynomial differential systems, *J. Fixed Point Theory Appl.*, **3** (2008), 331-351.

[9] S. Erlicher, A. Trovato, P. Argoul; Modeling the lateral pedestrian force on a rigid floor by a self-sustained oscillator, *Mech. Syst. Signal Pr.*, **24** (2010), 1579–1604.

[10] S. Erlicher, A. Trovato, P. Argoul; A modified hybrid van der Pol/Rayleigh model for the lateral pedestrain force on a periodically moving floor, *Mech. Syst. Signal Proc.*, **41** (2013), 481-501.

[11] A. C. de Pina Filho, M. S. Dutra; Application of hybrid van der Pol-Rayleigh oscillators for modeling of a bipedal robot, *Mech. Solid Braz.*, **1** (2009), 209-221.

[12] A. C. de Pina Filho, M. S. Dutra, L. Raptopoulos; Modeling of a bipedal robot using mutually coupled Rayleigh oscillators, *Biol. Cybern.*, **92** (2005), 1-7.

[13] P. Kumara, A. Kumara, S. Erlicher; A modified hybrid Van der Pol-Duffing-Rayleigh oscillator for modelling the lateral walking force on a rigid floor, *Phys. D*, **358** (2017), 1-14.

[14] N. Levinson, O. K. Smith; A general equation for relation oscillations, *Duke Math. J.*, **9** (1942), 382-403.

[15] J. Llibre, C. Valls; Global asymptotic stability in quadratic systems, *Electron. J. Differential Equations*, **2025** (2025), Paper No. 36, 12 pages.

[16] A. H. Nayfeh, B. Balachandran; *Applied Nonlinear Dynamics*, Wiley, Weinheim, 2004.

[17] L. Rayleigh; *The Theory of Sound*, Dover, New York, 1945.

[18] B. Van der Pol; On relaxation-oscillations, *Lond. Edinb. Dublin Phil. Mag. J. Sci.*, **2** (1927), 978-992.

[19] A. Venkatesan, M. Lakshmanan; Bifurcation and chaos in the double-well Duffing-van der Pol oscillator: Numerical and analytical studies, *Phys. Rev. E*, **56** (1997), 6321-6330.

[20] X. Yang, J. Zhou; Classification of boundary-equilibria for two-dimensional continuous piecewise linear systems with two intersecting switching lines, *Electron. J. Differential Equations*, **2025** (2005), Paper No. 42, 19 pages.

[21] Z. Zhang, T. Ding, W. Huang, Z. Dong; *Qualitative Theory of Differential Equations*, Transl. Math. Monogr., Amer. Math. Soc., Providence, RI, 1992.

Yuhuan Lu

School of Mathematics and Statistics, MNP-LAMA, Central South University, Changsha, Hunan 410083, China

Email address: lu_yuhuan@csu.edu.cn

Rui Zhang (corresponding author)

School of Mathematics and Statistics, MNP-LAMA, Central South University, Changsha, Hunan 410083, China

Email address: zhang_rui@csu.edu.cn